The Light-Induced "Worm" in Undergraduate Physical Chemistry

Michael A. Vaksman

Department of Chemistry, University of Wisconsin–Superior, Superior, WI 54880-2898, mvaksman@staff.uwsuper.edu

Abstract: We suggest a one-term course project based on a light-induced "worm" that can improve students' understanding of several major principles, such as the material-balance equation, light absorption, and line broadening in laser spectroscopy. A description of the effect of the light-induced worm is presented along with the results for a trial run of the project and plans for future enhancements.

Probably every instructor has observed the difficulties that students have with the material-balance equation [1]:

$$\frac{\partial N}{\partial t} = D\frac{\partial^2 N}{\partial x^2} - \upsilon\frac{\partial N}{\partial x} - kN \qquad (1)$$

where N is the concentration of a gas, D is the diffusion coefficient, υ is the rate of convection, and k is the rate constant for a pseudo-first-order reaction. Consider, for example, the following simple problem:

> Gas A in a reactor undergoes chemical decomposition in a pseudo-first-order reaction with a rate constant, k, of 50 s^{-1}. There are three gauges installed inside the reactor to monitor the concentrations of the gas: (1) near the wall, (2) 1 cm from the wall, and (3) 2 cm from the wall. Initially, the concentrations of A are: 0 near the wall, 1.0×10^{10} cm^{-3} at 1 cm from the wall, and 1.5×10^{10} cm^{-3} at 2 cm from the wall. There is a noble gas (in addition to the reactant A) in the reactor; its concentration, N_b, is 1×10^{18} cm^{-3}. The thermal velocity, υ_T, is 1×10^5 cm s^{-1} and the collision cross section, σ, is 1×10^{-15} cm^2. Estimate the rate of change of the concentration of A at a distance of 1 cm from the wall. Neglect convection.

Many students don't feel comfortable either with the physics of the related transfer phenomena or with evaluating the partial derivatives. The idea that the value of a partial derivative can be estimated using the simple equalities (equation 2) common in numerical analysis,

$$\frac{\partial^2 N}{\partial x^2} = \frac{\partial}{\partial x}\left(\frac{\partial N}{\partial x}\right) \cong \frac{\frac{N_{i+1}-N_i}{\Delta x} - \frac{N_i - N_{i-1}}{\Delta x}}{\Delta x} = \frac{N_{i+1} - 2N_i + N_{i-1}}{(\Delta x)^2} \qquad (2)$$

is foreign to them. Because the material-balance equation (equation 1) is of central importance in chemical kinetics, the situation must be rectified.

Recently, there have been numerous suggestions aimed at improving the teaching of chemical kinetics (see, for example, references 2–4). We propose to deepen students' understanding of its principles through a course project in which they study the light-induced "worm," an interesting effect that can arise in a gas under laser excitation. Just as spinodal decomposition allows the illustration of several important concepts in chemical thermodynamics [5], the light-induced worm provides similar opportunities for chemical kinetics. The light-induced worm is an effect with a rare combination of teaching advantages. First, it is a spectacular phenomenon that inspires the desire of any good student to understand it, and, second, due to its clear physics, it can indeed be quite easily understood by such a student.[1] Besides providing an occasion to utilize the material-balance equation, this project gives students the opportunity to work with the differential form of the Beer–Lambert Law, which is also an important topic (See references 6 and 7), and to thoroughly examine several major principles of laser spectroscopy [8]. Below, we describe the content of the suggested project and recommend a time frame for its execution. We start by describing the surface light-induced-drift phenomenon that enables the light-induced worm to move.

Surface Light-Induced Drift

Surface light-induced drift (SLID) occurs at the intersection of three areas of physical chemistry: laser spectroscopy, gas kinetics, and surface science. In SLID studies (Figure 1a), a laser beam travels through a cell containing a rarefied gas, its frequency, ω, slightly tuned off a molecular frequency, ω_0. Consider the case of a monochromatic laser beam where the homogeneous width of the excited state is small compared to the Doppler broadening [8]. Due to the Doppler effect, the laser excites only molecules with an x projection of their velocity around $\upsilon_0 = (\omega - \omega_0)/k$, where x is the direction of the laser beam, and k is the radiation wave vector (velocity-selective excitation). Now, consider the scattering of the molecules by the walls of the cell. To describe the transfer of parallel momentum of the molecules to the wall, we introduce the accommodation coefficient a:

$$a \equiv \frac{\left\langle\left|\upsilon_{out}\right|\right\rangle - \left\langle\left|\upsilon_{inc}\right|\right\rangle}{\left\langle\left|\upsilon_{inc}\right|\right\rangle}$$

where $\left\langle\left|\upsilon_{inc}\right|\right\rangle$ and $\left\langle\left|\upsilon_{out}\right|\right\rangle$ are the average magnitudes of the longitudinal components of the velocities of the incident molecules and of the scattered molecules correspondingly. The

[1] We are grateful to a reviewer for this remark.

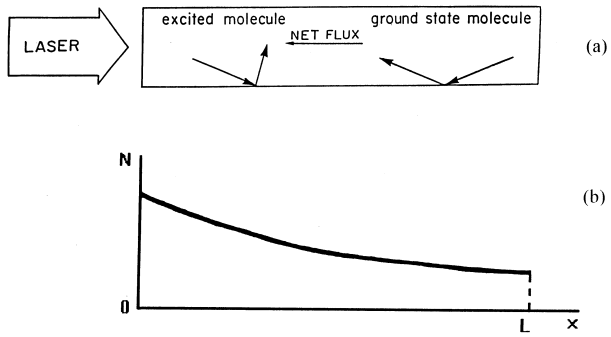

Figure 1. (a) The origin of SLID flux. Laser-radiation frequency is shifted to the blue ($\omega > \omega_0$), accommodation coefficient in the excited state is larger than in the ground state ($\Delta A > 0$). (b) The density gradient arising in a cell with closed ends due to the SLID flux.

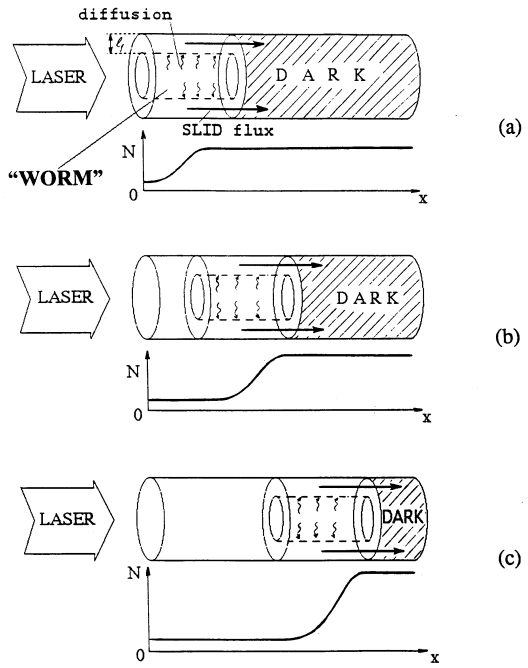

Figure 2. The light-induced "worm". Figures (a), (b), and (c) represent three consecutive positions of the "worm" as it moves from the irradiated end of the cell toward the dark end. The graphs *N(x)* show the corresponding profiles of the concentration of the resonant gas along the cell.

values of *a* in the excited and in the ground state are generally not equal. For vibro-rotational excitation of molecules, for example, the change of *a* can be caused by the transition of part of the energy of excitation into translational energy. In the case of electronic excitation of atoms, the change of *a* can occur due to the change of the polarizability of an atom and the resulting change in the energy of its interaction with the surface. Let the value of *a* be higher for molecules excited by laser radiation than for nonexcited ones. The molecules in the excited velocity group around υ_0 will then be attenuated by the cell walls more efficiently than molecules in the opposing velocity group (around $-\upsilon_0$). This gives rise to a net flux, SLID flux (see Figure 1a). SLID was predicted in our papers [9–11], observed experimentally soon thereafter [12–15], and has remained the main subject of my studies since then [16–24].

The magnitude of the SLID flux, *j*, is proportional to the difference, Δa, between the accommodation coefficients for the excited and the nonexcited molecules and to the density N_e of excited molecules: $j \sim -\Delta a\, N_e\, \upsilon_0$. Because N_e, in turn, is proportional to the absorption of the laser radiation, $N_e \sim dI/dx$, the SLID flux, *j*, is also proportional [11, 16] to *dI/dx*:

$$\upsilon_{SLID} N \equiv j = \frac{\Delta a}{a_g} \frac{\upsilon_0}{h\omega\left(\gamma + \nu_g\right)} \frac{dI}{dx} \qquad (3)$$

where υ_{SLID} is the velocity of the SLID flux, $\upsilon_{SLID} \equiv j/N$; *N* is the density of the gas; $\Delta a \equiv a_e - a_g$, where the subscripts *e* and *g* correspond to the molecules in the excited state and in the ground state, respectively; γ is the Einstein coefficient of spontaneous emission; and ν_g is the frequency of velocity-randomizing collisions of the ground-state molecules. If the laser radiation intensity, *I*, is small, then *dI/dx* is small; and thus, according to equation 3, the SLID flux, *j*, is also small.

In a closed cell the SLID flux must be compensated by a diffusive flux, which leads to the increase of the molecular density at the end of the cell where the SLID flux is directed (Figure 1b). The resulting relative pressure drop along the cell is then

$$\frac{\Delta P}{P} \approx \left(\frac{\upsilon_{SLID}}{\upsilon_T}\right)\left(\frac{L}{R}\right)$$

where υ_T is the thermal velocity, *L* is the cell length, and *R* is its radius. The factor *L/R* above can be as large as 103 in real experimental conditions. That is why SLID is exceedingly sensitive to changes in molecule-surface interactions with excitation. Even in cases where Δa is very small, substantial *L/R* can lead to a measurable pressure drop [9–15].

SLID can also cause appreciable fluxes and density gradients in a cell with a dense gas or a mixture of resonant and buffer gases where the particle mean free path, l_f, is much smaller than the cell radius [11]. The reason is that in a narrow layer of a thickness l_f near the wall, collisions with other particles do not yet decelerate the SLID flux created by the surface scattering, and the SLID flux in this area remains rapid.

SLID can be used as a method to study gas–surface interactions and heterogeneous catalysis and possibly as a tool for isotope separation [9–20]. Besides its fundamental significance, SLID is attractive as a subject for undergraduate research because it is so well structured and small "local" problems can be identified that are feasible for undergraduates. (See, for example, references 22 and 24).

The Light-Induced "Worm"

The Nature of the Effect. In the above discussion, it was implied that the cell containing the gas is short enough for the laser beam to penetrate the whole cell without a decrease of its intensity. Let us consider now a different case. Suppose that the cell is very long, so that the laser radiation is totally

absorbed at a short distance from the cell entrance as compared to the overall cell length. What will happen in the cell now?

The answer to this question depends upon the direction of the SLID flux. If it is directed *toward* the laser beam (as in Figure 1), the changes will be minimal, only the gas density near the cell entrance will rise somewhat. Deeper into the cell, the radiation intensity, I, and therefore the absorption, dI/dx, and υ_{SLID}, remain negligible (see equation 3). Fortunately, it is easy to change the direction of the SLID flux. To do this, it is enough to change the sign of the detuning $(\omega - \omega_0)$ of the laser frequency, ω, with respect to the molecular frequency, ω_0. Then, the molecules will be excited, not in the velocity interval around υ_0, but in the interval around $-\upsilon_0$. As a result, the direction of the SLID flux will be switched, and the resonant molecules will start to move *away* from the cell entrance (Figure 2a). This case is much more interesting. Soon after the laser is switched on, the area near the cell entrance becomes depleted of the resonant molecules as they drift away, and the laser radiation can penetrate deeper into the cell to initiate SLID flux there. It causes creation of void space in a longer area, enabling the radiation to penetrate even deeper, and so on. This "positive feedback" between the spreading radiation and gas-density profiles will ultimately lead to the gas molecules concentrating with a relatively high density at the "dark" end of the cell (Figure 2). Because the gas moves due to its interaction with the cell walls, resembling in a sense a worm's crawling, we have called this phenomenon light-induced worm [19]. Of all the effects induced by SLID, light-induced worm seems the most fascinating to undergraduate students when it is described during a lecture on laser spectroscopy.

Numerical Analysis. The derivation of the equations that describe the worm's movement is normally beyond the capabilities of an undergraduate student. The resulting equations themselves (at least for the case of a rarefied gas that we consider here), however, are quite simple, and their physical meaning is clear. To assist students in mastering the background material, a concise handout containing the description of the effect and the main formulas has been prepared.

We start with equation 4, which controls the evolution of the density, N, of the rarefied gas:

$$\frac{\partial N}{\partial t} = D\frac{\partial^2 N}{\partial x^2} - \frac{\partial\left(\upsilon_{SLID} N\right)}{\partial x} - kN \qquad (4)$$

Here k is a constant characterizing the adsorptive properties of the cell-wall surface. As one can see, equation 4 is the material-balance equation (equation 1), where the rate of convection, υ, has been replaced by the rate of υ_{SLID}, of the SLID flux. Thus, for the purpose of the student project described here, we can think of SLID as a kind of "stimulated convection." Notice that diffusion perpendicular to the laser beam can be neglected here because we are considering the case of a rarefied (Knudsen) gas, where the particle's mean free path is larger than the diameter of the cell. In other words, molecules fly from one wall to another in the transverse direction without experiencing intermolecular collisions. When we consider a dense gas (see below), the transverse diffusion indeed needs to be considered; this is the main difference that makes a similar problem treating a dense gas more difficult.

The equation that describes the light absorption along the cell is a generalization of the differential form of the Beer–Lambert equation:

$$\frac{\partial I}{\partial x} = -\sigma N(x) I(x) \qquad (5)$$

where σ is the effective absorption cross section of the resonant atoms. When the laser intensity, I, approaches the saturation intensity, I_{sat}, a large fraction of the molecules is promoted to the excited state and will not absorb radiation. Because of this, the magnitude of σ decreases as I approaches I_{sat}. For electronic transitions, $I_{sat} \sim 10$ W cm^{-2}.

Finally, we describe the equation that relates the magnitude of the SLID velocity at a particular point along the cell, $\upsilon_{SLID}(x,t)$, to the light intensity and the gas density at that point, $I(x,t)$ and $N(x,t)$. We already have such an equation; it is equation 3, which we present here again as equation 6:

$$\upsilon_{SLID}\left(x,t\right) N\left(x,t\right) = \frac{\Delta a}{a_g}\frac{\upsilon_0}{h\omega\left(\gamma + v_g\right)}\frac{dI\left(x,t\right)}{dx} \qquad (6)$$

Equations 4–6 represent a complete set of equations that fully describe the evolution of this system—the movement of the worm. They are similar to the set of equations that describe the similar phenomenon of the light-induced "piston" [25–29]. The difference between the light-induced worm and light-induced piston is in the mechanism of the movement of the gas. While in the former case it is SLID, in the latter case it is bulk light-induced drift [25] where the role of the cell walls in initiating the drift is played by the particles of a buffer gas. Analytical solution of the system of equations 4–6 is possible only for an *infinitely* long cell [27–29]. For this project, the students perform numerical analysis of the worm in a cell with a *finite* length. Analysis of the above equations and the corresponding literature takes the students three weeks. Equations 4–6 need to be supplemented with the boundary conditions for the ends of the cell. We assume, for example, that there is no adsorption of the gas molecules by the lateral walls. Then, the sum of the SLID flux and the diffusional flux at each end of the cell must be zero.

$$-\upsilon_{SLID} N\Big|_{x=0,L} + D\frac{\partial N}{\partial x}\Big|_{x=0,L} = 0 \qquad (7)$$

The next step is to normalize the variables in equations 4–6 in order to avoid operating with numbers that are too large or too small as compared to 1. Although this procedure is common in numerical analysis, students find it the most difficult part of the project. (Because performing the normalization is not essential for the students to gain an understanding of the physical principles behind the project, providing the students with the normalized set of equations along with equations 4–6 has been considered.)

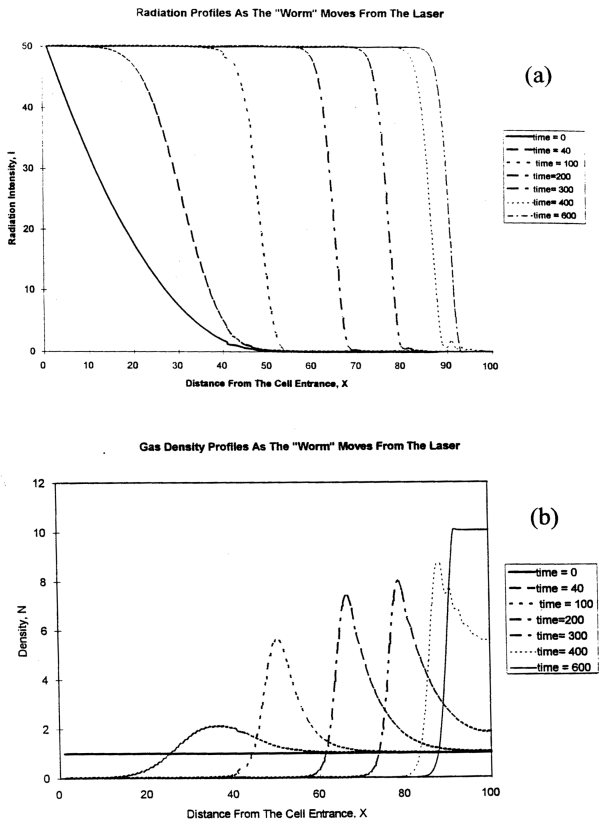

Figure 3. The result of the numerical simulation of the "worm" 's movement: (a) the radiation intensity profiles, (b) the gas density profiles for several consecutive moments as the "worm" moves to the dark end of the cell.

Substitution of equations 8

$$\tilde{N} \equiv \frac{N}{N_0}, \quad \tilde{\upsilon}_{SLID} \equiv \frac{\upsilon_{SLID}}{\upsilon_T}, \; \tilde{I} \equiv \frac{I}{I_{sat}}, \quad \tilde{x} \equiv \frac{x}{R}, \quad \tilde{t} \equiv t\frac{\upsilon_T}{R} \quad (8)$$

into equations 4–6 gives equations 9–11.

$$\frac{\partial \tilde{N}}{\partial \tilde{t}} = \frac{\partial^2 \tilde{N}}{\partial \tilde{x}^2} - \frac{\partial\left(\tilde{\upsilon}_{SLID}\,\tilde{N}\right)}{\partial \tilde{x}} \quad (9)$$

$$\frac{\partial \tilde{I}}{\partial \tilde{x}} = -q\frac{\tilde{I}(x,t)}{\left[1+\tilde{I}(x,t)\right]^{0.5}}N(x,t) \quad (10)$$

$$\tilde{\upsilon}_{SLID}(x,t)\,N(x,t) = p\frac{\partial \tilde{I}(x,t)}{\partial \tilde{x}} \quad (11)$$

where N_0 is the initial concentration of the gas in the cell, $q \equiv R\sigma_0 N_0$, $p \equiv \Delta a(2R\sigma_H N_0)$–1, and $\sigma_H \equiv \hbar\,\omega\,(\gamma + v_g)/(2\,I_{sat})$. We have neglected adsorption (k = 0) and assumed $\sigma \approx \sigma_0\,(1 + I/I_{sat})0.5$ [27]. The boundary condition (7) now takes the form of equation 12 below:

$$-\tilde{\upsilon}_{SLID}\tilde{N}\Big|_{\tilde{x}=0,L} + \frac{\partial \tilde{N}}{\partial \tilde{x}}\Big|_{\tilde{x}=0,L} = 0 \quad (12)$$

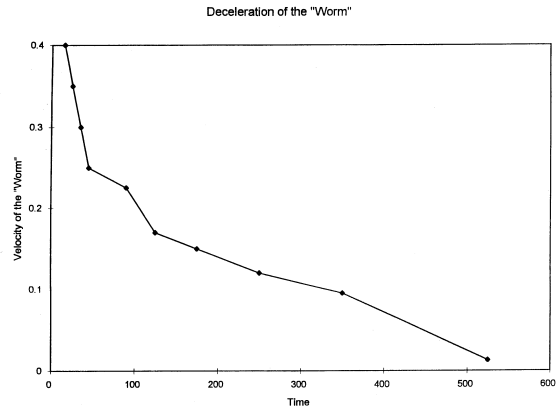

Figure 4. The velocity of the "worm" as a function of time, according to the results of Figure 3.

The algorithm for the numerical solution of equations 9–11 was written by a student in about one month. An excellent book, *Numerical Recipes in FORTRAN: The Art of Scientific Computing* [30], can be recommended for a thorough introduction of the skills of finite differencing and FORTRAN programming. A simple explicit scheme for the solution of a set of partial differential equations has been implemented, where all the derivatives in each partial differential equation are replaced by the finite differences (similar to equation 2), and the values of N, I, and υ_{SLID} at each subsequent moment of time are calculated from the corresponding values at the previous moment [30]. The program developed by the student is presented in the Appendix.

It took another month for the student to debug the program and start to obtain sensible numerical results. An example of these results is given in Figure 3. Notice the correlation between the advancement of the radiation front (Figure 3a) and the movement of the region of high gas density (Figure 3b). From these results, the student was able to deduce original conclusions. For example, according to the analytical results for an infinite cell, the velocity of the movement of the region of high gas density is constant [27, 28]; however, for a finite cell it was found that the velocity is monotonously decreasing with time (Figure 4).

At each stage of the project, the students are encouraged to think about the physical meaning of the results produced by the computer. They are asked, for instance, "Why do you think the region of high density in Figure 3b is forming?" (Answer: SLID pushes the gas to the right. As the radiation intensity in this area is small, subsequent transport of the gas to the dark region of the cell can be done only by diffusion. Because the rate of diffusion is $-D\,dN/dx$ [1], an appreciable negative gradient of the density is needed. Because the concentration of the gas in the dark region is almost N_0, a region of high density $N > N_0$ *must* exist to provide the needed negative gradient of the density). And, "Which region along the cell do you expect to be fluorescing during the worm's movement?" (Answer: The front of the worm (the region of maximal N) is fluorescing. To the left of the front, there is *no gas* to absorb the radiation and to fluoresce; deep to the right of the front, there is *no radiation* to be absorbed and re-emitted.) The students can be shown the spectacular series of photographs [26, 29] (Figure 5) depicting the movement of the light-

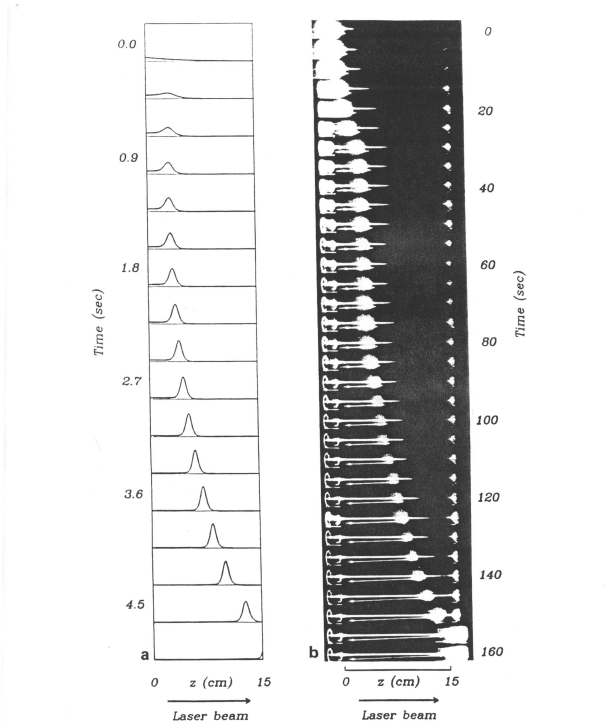

Figure 5. Experimental data on the travel of the light-induced piston through the capillary cell. (Reproduced from reference 29 with premission from Elsevier Science.)

induced piston in the system containing irradiated gaseous sodium atoms in a buffer gas [31].

Finally, this student project has initiated plans, which are described below, for future research. Several more-complicated cases of the light-induced worm will be considered. These arise in a dense resonant gas or in a mixture of a resonant and a buffer gas. In the latter case, both the bulk light-induced diffusion (LID) [25] and the SLID can arise simultaneously. In particular, cases in which the directions of LID and SLID fluxes are anticollinear are noteworthy. In this situation, one would expect existence of threshold values of Δa below which the worm can not arise. Determination of certain parameters of the worm, such as front steepness and velocity, can provide sufficient information to determine the state dependence of the surface accommodation coefficients, a, versus the buffer-gas pressure. Quantitative analysis in this situation is more complicated than in the case of a LID piston [27–29] and the case of SLID in a rarefied gas presented above where the problem could be reduced to one dimension. Also, adsorption can be taken into consideration in a way similar to that in reference 32. We will have undergraduate students actively involved in this stage of the project as well.

In conclusion, we suggest a one-term course project in physical chemistry that can improve the students' understanding of several major principles, such as the material-balance equation, light absorption, and line broadening in laser spectroscopy. The time frame of the project is as follows: (1) analysis of the equations and the corresponding literature, three weeks with one hour per week of discussions with the instructor and two more hours per week of independent work; (2) writing of the algorithm for the numerical solution of the equations, approximately one month; (3) debugging the program and obtaining sensible numerical results, one month. The project was implemented last year. In the coming year, it will be offered as an extra-credit project. Assigning it as a group project (to groups of 2–3 students) may also be beneficial. For this project, it is easy to generate assignments that will bear little resemblance to each other in their output. For instance, if the boundary condition (equation 7) is replaced by the requirement that the gas densities at the cell ends remain constant, (which can be done experimentally by attaching those ends to large reservoirs containing the resonant gas), the resulting density profiles are nearly triangular in shape with the apex near the cell entrance or exit, dependent upon the initial optical thickness, $N_0 \sigma_0 L$ [26, 29], and thus have little in common with the results depicted in Figure 3b. Additional variation can be created by changing the values of the coefficients, p and q, describing the magnitudes of the radiation intensity and the SLID flux, respectively. Variation of these coefficients changes both the steepness of the worm's front and the speed of its movement.

Appendix

```
PARAMETER (XX=100    ,TT=101)
    DIMENSION AN(XX,TT),AI(XX,TT),v(XX,TT),SUM(TT)
    INTEGER x,t
    REAL p,q,dt,dx
    OPEN (UNIT=I ,FILE="MYDATA",STATUS="NEW")
c   x=position, t=time
    p=-O.3
    q=O.3
    dt=.l
10  dx=l.
c   Loop to define all concentrations the same, and v=O at t=1
    DO x=1 ,XX
    AN(x,1)=1.
    v(x,1)=O.
    END DO
c   Loop to define laser intensity to be 50 at all x=l
    DO t=l ,TT
    Al(1,t)=50.
    END DO
c   Loop for finding all intensities at t=1
21  DO x=1,XX-1
    Al(x+1,1)=-q*AI(x,1)/(SQRT(1.+AI(x,1)))*AN(x,1 )+Al(x,1)
```

```
    END DO
c   Loops for finding intensities, velocities and concentrations
    do co=0,100
    DO t=1,TT-1
    DO x=2,XX-1
27     AN(x,t+1)=(((AN(x+1,t)-(2.*AN(x,t))+AN(x-1,t))/(dx*dx))
   +   -((v(x+1,t)*AN(x+1,t)-(v(x,t)*AN(x,t)))/dx))*dt+AN(x,t)
29     AI(x,t+1)=-q*AI(x-1,t+I)/(SQRT(1.+AI(x-1,t+1)))*AN(x,t+1)
   +   +AI(x-1,t+l)
         IF (AI (x,t+1).LT.0.) AI(x, t+1)=0.
         v(x,t+1)=-q*p*(AI(x,t+1)/(SQRT(1.+AI(x,t+l))))
         END DO
         AI(XX,t+1)=-q*AI(XX-1,t+1)/(SQRT(1.+AI(XX-1,t+1)))*AN(XX-1
   +    ,t+l) +AI(XX-I,t+1)
         v(1,t+1)=-q*p*(AI(1,t+1)/(SQRT(1.+AI(1,t+l))))
         v(XX,t+1)=-q*p*(AI(XX,t+1)/(SQRT(1.+AI(XX,t+1))))
         AN(1,t+1)=AN(2,t+1)*(1-v(1,t+1))
         AN(XX,t+1)=AN(XX-1,t+1)/(1-v(XX,t+1))
         SUM(t+1)=0.
          DO x=2,XX-1
           SUM(t+1)=SUM(t+1)+AN(x,t+1)
          END DO
         SUM(t+1)=SUM(t+1)+(AN(1,t+1)+AN(XX,t+1))/2.
    END DO
    DO t=1,TT,101

        TIME = co*dt*(TT-1) + dt*(t-1)
        WRITE (1,*)'time=',TIME
      DO x=1,XX
         WRITE (1,99) AN(x,t),AI(x,t),v(x,t)
99        FORMAT(3X,3(G16.4,3X))
 END DO
     WRITE (1,*) 'SUM=',SUM(t+1)
 END DO
   do x=1,XX
      AI(x,1)=AI(x,TT)
      AN(x,1)=AN(x,TT)
      v(x,1)=v(x,TT)
   end do
end do
END
```

References

1. Atkins, P. W. *Physical Chemistry*, 5th ed.; Freeman: New York, 1994; Section 27-3.
2. Pojman, J. *J. Chem. Educ*. **1990**, *67*, 200.
3. Tagg, S. L.; LeMaster, C. L.; LeMaster, C. B.; McQuarrie, D. A. *J. Chem. Educ*. **1994**, *71*, 363.
4. Tan, X.; Lindenbaum, S.; Meltzer, N. *J. Chem. Educ*. **1994**, *71*, 566.
5. Clerc, D. G.; Cleary, D. A. *J. Chem. Educ*. **1995**, *72*, 112.
6. Lykos, P. D. A. *J. Chem. Educ*. **1992**, *69*, 730.
7. Light, L. B.; Huebner, J. S.; Vergenz, R. A. *J. Chem. Educ*. **1994**, *71*, 105.
8. Atkins, P. W. *Physical Chemistry*, 5th ed.; Freeman: New York, 1994; Chapters 16 and 17.
9. Ghiner, A. V.; Stockmann, M. I.; Vaksman, M. A. *Phys. Lett*. **1983**, *96A*, 79.
10. Vaksman, M. A. Phys. Chem. & Mech. Surf. (Great Britain) **1985**, 3, 3222.
11. Vaksman, M. A.; Ghiner, A. V. *Sov. Phys. JETP*, **1985**, *62*, 23.
12. Hoogeveen, R. W. M.; Spreeuw, R. J. C.; Hermans, L. J. F. *Phys. Rev. Lett*. **1987**, *59*, 447.
13. Hoogeveen, R. W. M., van der Meer, G. J.; Hermans, L. J. F. *Phys. Rev*. **1990** *A42*, 6471.
14. van der Meer, G. J.; Broers, B.; Hoogeveen, R. W. M.; Hermans, L. J. F. *Physica* **1992** *A182*, 47.
15. Broers, B.; van der Meer, G. J.; Hoogeveen, R. W. M.; Hermans, L. J. F. *J.Chem. Phys*. **1991**, *95*, 648.
16. Vaksman, M. A. *Phys. Rev.* **1991**, *A44*, 3125.
17. Vaksman, M. A. *Phys. Rev.* **1991**, *A44*, **R**4102.
18. Vaksman, M. A. *Phys. Rev*. **1993**, *A48*, **R**26.
19. Vaksman, M. A.; Ben-Reuven, A. *Phys. Rev*. **1992**, *A45*, 7883; Vaksman, M. A.; Ben-Reuven, A. Surface Light-Induced Drift as a Tool to Study Gas-Surface Interactions. Presented at the 12th International Vacuum Congress/8th International Conference on Solid Surfaces, The Hague, The Netherlands, October 1992; *Surf. Sci*. **1993**, *287/288*, 196.
20. Vaksman, M. A. *Phys. Rev*. **1995**, *A52*, 2179.
21. Vaksman, M. A. *Phys. Rev*. **1996**, *A54*, 3270.
22. Vaksman, M. A.; Podgorski, I. *Can. J. Phys*. **1996**, *74*, 251.
23. Vaksman, M. A. *Chem. Phys. Lett.* **1997**, *267*, 77.
24. Vaksman, M. A.; Dahl, J. L. *Can. J. Phys*., in press.
25. Gelmukhanov, F. Kh.; Shalagin, A. M. *Sov. Phys. JETP* **1980**, *51*, 839.
26. Werij, H. G. C.; Woerdman, J. P.; Beenakker, J. J. M.; Kuscer, I. *Phys. Rev. Lett*. **1984**, *52*, 2237.
27. Nienhuis, G. *Phys. Rev*. **1985**, *A31*, 1636.
28. Nienhuis, G. *Phys. Rep*. **1986**, *138*, 152.
29. Werij, H. G. C.; and Woerdman, J. P. *Phys. Rep.* **1988**, *169*, 145.
30. Press, W. H.; Teukolsky, S. A.; Vetterling, W. T.; Flannery, B. P. *Numerical Recipes in FORTRAN: The Art of Scientific Computing*, 2nd ed.; Cambridge University Press: Cambridge, MA, 1992, Chapter 19.
31. The experiment [29] has been performed on sodium vapor contained in a paraffin-coated narrow tube using a narrow-band dye laser (Spectra Physics 380D) as a light source. The cell has been also filled with a noble gas at a pressure in the range 1–10 torr.
32. Nienhuis, G. *Optics Comm.* **1987**, *62*, 81.